

# NJL-model description of Goldstone boson condensation in the color-flavor locked phase

Michael Buballa

*Institut für Kernphysik, TU Darmstadt, Schlossgartenstr. 9, 64289 Darmstadt, Germany*

## Abstract

A schematic NJL-type model is employed to investigate kaon and pion condensation in deconfined quark matter in the color-flavor locked (CFL) phase, explicitly referring to quark degrees of freedom. To that end we allow for non-vanishing pseudoscalar diquark condensates in addition to the scalar ones which constitute the CFL phase. Color neutrality is ensured by the appropriate choice of color chemical potentials. The dependence of the free energy in the Goldstone condensed phases on quark masses and charge chemical potentials is found to be in good qualitative – in most cases also quantitative – agreement with the predictions obtained within the effective Lagrangian approach.

## 1 Introduction

It is now generally believed that strongly interacting matter at low temperatures and very high densities is a color superconductor in the color-flavor locked (CFL) phase [1, 2, 3, 4] (For reviews on color superconductivity see, e.g., Refs. [5, 6, 7, 8]). For vanishing quark masses this phase can be characterized by the equality of three scalar diquark condensates in the color and flavor antitriplet channel,

$$s_{22} = s_{55} = s_{77} , \quad (1)$$

where

$$s_{AA'} = \langle q^T C \gamma_5 \tau_A \lambda_{A'} q \rangle . \quad (2)$$

Here  $q$  is a quark field, and  $\tau_A$  and  $\lambda_{A'}$ ,  $A, A' \in \{2, 5, 7\}$ , denote the antisymmetric Gell-Mann matrices acting in flavor space and color space, respectively. In general, these condensates are accompanied by induced color-flavor sextet condensates, which are, however, small and will be neglected in this article.

The condensates Eq. (1) break the original  $SU(3)_{color} \times SU(3)_L \times SU(3)_R$  symmetry of QCD (in the chiral limit) down to a residual  $SU(3)_{color+V}$ , corresponding to a common (“locked”) rotation in color and flavor space. As a consequence of the breaking of the color symmetry, all eight gluons receive a mass, while the breaking of chiral symmetry leads to the emergence of eight pseudoscalar Goldstone bosons. The latter reflect the fact

that there is a continuous set of degenerate ground states which can be generated from the CFL ansatz, Eq. (1), via axial flavor transformations

$$q \longrightarrow \exp(i\theta_a \frac{\tau_a}{2} \gamma_5) q, \quad a = 1, \dots, 8. \quad (3)$$

Under these transformations the scalar diquark condensates, Eq. (2), are partially rotated into pseudoscalar ones,

$$p_{AA'} = \langle q^T C \tau_A \lambda_{A'} q \rangle. \quad (4)$$

These condensates are expected to become relevant when we consider the less perfect but more realistic situation where chiral symmetry is explicitly broken through non-zero quark masses or external charge chemical potentials. In this case the CFL state can become unstable against developing non-zero values of  $p_{AA'}$ , corresponding to pion or kaon condensation [9, 10, 11].

This behavior has been predicted within low-energy effective field theories which can be constructed systematically for excitations much smaller than the superconducting gap  $\Delta$  [9, 10, 11, 12, 13, 14]. Basically, this is Chiral Perturbation Theory ( $\chi$ PT) with the essential difference to the well-known  $\chi$ PT at low densities that at high densities the interaction is weak and the coefficients can be calculated from QCD within High Density Effective Field Theory [10, 15, 16], which is valid for energies much smaller than the chemical potential.

Let us briefly summarize the leading-order results which we need for later comparison. Adopting the notation of Ref. [11], the effective meson masses are given by

$$M_\pi^2 = 2a m_q m_s, \quad M_K^2 = a(m_q + m_s) m_q, \quad (5)$$

where we have assumed equal masses for the light quarks,  $m_u = m_d =: m_q$ . At asymptotic densities, the coefficient is given by  $a = 3\Delta^2/(\pi^2 f_\pi^2)$  [12], where  $\Delta$  is the CFL gap and the pion decay constant is given by  $f_\pi^2 = (21 - 8 \ln 2)\mu^2/(36\pi^2)$ .

The mesons experience effective chemical potentials

$$\tilde{\mu}_{\pi^+} = \mu_Q, \quad \tilde{\mu}_{K^+} = \mu_Q + \frac{m_s^2 - m_q^2}{2\mu}, \quad \tilde{\mu}_{K^0} = \frac{m_s^2 - m_q^2}{2\mu}, \quad (6)$$

and the same with the opposite signs for  $\pi^-$ ,  $K^-$ , and  $\bar{K}^0$ . The above expressions imply that meson condensation takes place if  $\tilde{\mu}_i$  exceeds the mass of the corresponding meson. In this case the thermodynamic potential of the system is lowered by

$$\delta\Omega_i = -\frac{f_\pi^2}{2} \tilde{\mu}_i^2 (1 - \cos\theta)^2, \quad \cos\theta = \frac{M_i^2}{\tilde{\mu}_i^2}, \quad (7)$$

while for  $\tilde{\mu}_i^2 < M_i^2$  the CFL state is stable, i.e.,  $\theta = 0$ .

Note that the above expressions are of order zero in  $\alpha_s$ . They are therefore universal in the sense that they should not only hold in QCD, but in any model with the same symmetry pattern, as long as higher-order corrections in the interaction are small.

Aim of the present article is to study this mechanism and the corresponding CFL + Goldstone phases within a schematic NJL-type model, explicitly referring to the diquark condensates  $s_{AA'}$  and  $p_{AA'}$ . Our main motivation is the fact that NJL-type models

have successfully been used to investigate various color superconducting phases and their competition (see Ref. [17] and references therein), but so far the possibility of Goldstone boson condensation has not been taken into account\*. In particular the recently proposed gapless phases at densities below the CFL regime [19, 20, 21] have only been studied within NJL-type models which neglect Goldstone condensates. In the present paper we want to lay a basis for a more complete analysis in the future. We thereby focus on the general mechanism. We investigate whether and under which conditions Goldstone condensation takes place in NJL-type models and compare the results with the predictions of the effective theories. To keep the analysis as simple as possible we do not consider  $\bar{q}q$  and  $\bar{q}i\gamma_5\tau_a q$  condensates at the present stage. An extension of the model in this direction is straight forward.

## 2 Chiral transformations

Before we define our model we should discuss the axial transformations introduced in Eq. (3) in some more details. In this article we consider exclusively flavor non-diagonal modes of Eq. (3). According to their quantum numbers, these modes can be identified with charged pions (“ $\pi^\pm$ ”,  $a = 1, 2$ ), charged kaons (“ $K^\pm$ ”,  $a = 4, 5$ ), or neutral kaons (“ $K^0$ ”,  $a = 6, 7$ ).

As mentioned earlier, under these transformations the scalar diquark condensates are partially rotated into pseudoscalar ones. For a  $K^0$  mode, for instance, the transformed condensates read

$$\begin{aligned}
K^0 : \quad s'_{22} &= \cos \frac{\theta}{2} s_{22} & p'_{52} &= i \sin \frac{\theta}{2} (\hat{\theta}_6 - i\hat{\theta}_7) s_{22} \\
s'_{55} &= \cos \frac{\theta}{2} s_{55} & p'_{25} &= i \sin \frac{\theta}{2} (\hat{\theta}_6 + i\hat{\theta}_7) s_{55} \\
s'_{77} &= s_{77}
\end{aligned} \tag{8}$$

where  $\theta = \sqrt{\theta_6^2 + \theta_7^2}$  and  $\hat{\theta}_a = \theta_a/\theta$ . The primed and unprimed condensates refer to the values in the transformed state and in the original CFL state, respectively. Similarly, under  $K^\pm$  transformations,  $s_{22}$  and  $s_{77}$  are partially rotated into  $p_{72}$  and  $p_{27}$ , respectively, while  $\pi^\pm$  transformations, rotate  $s_{55}$  into  $p_{75}$  and  $s_{77}$  into  $p_{57}$ .

For equal quark masses, because of the residual  $SU(3)_{color+V}$  symmetry of the CFL state, the same combination of diquark condensates could be reached via axial *color* transformations

$$q \longrightarrow \exp(i\theta_a \frac{\lambda_a^T}{2} \gamma_5) q, \quad a = 1, \dots, 8. \tag{9}$$

---

\*For a recent NJL-model analysis of pion and kaon condensation in color non-superconducting quark matter, see Ref. [18].

For instance, for  $a = 6, 7$ , this transformation yields

$$\begin{aligned}
K'^0 : \quad s'_{22} &= \cos \frac{\theta}{2} s_{22} & p'_{25} &= i \sin \frac{\theta}{2} (\hat{\theta}_6 + i\hat{\theta}_7) s_{22} \\
s'_{55} &= \cos \frac{\theta}{2} s_{55} & p'_{52} &= i \sin \frac{\theta}{2} (\hat{\theta}_6 - i\hat{\theta}_7) s_{55} \\
s'_{77} &= s_{77} & &
\end{aligned} \tag{10}$$

Hence, as long as Eq. (1) holds exactly, both transformations, Eq. (8) and Eq. (10), lead to the same state. On the other hand, in the more realistic case of unequal quark masses, there is no exact flavor  $SU(3)_V$  to begin with and, thus, no exact  $SU(3)_{color+V}$  in the CFL phase. In this case the scalar diquark condensates  $s_{22}$ ,  $s_{55}$ , and  $s_{77}$  are in general not equal and the results of an axial flavor transformation and the corresponding axial color transformation will be different. Therefore, in order to distinguish between these two transformations, we indicate axial color transformations by a prime, i.e.,  $\pi'^{\pm}$ ,  $K'^{\pm}$ , and  $K'^0$ .

Looking at Eqs. (8) and (10) one might think that a maximally meson condensed state corresponds to a transformation angle  $\theta = \pi$ , i.e., when two of the three scalar diquark condensates are rotated away completely, and the two pseudoscalar diquark condensates receive their maximum value. This is, however, not true. To see this, it is instructive to perform an axial transformation on an idealized vacuum state with  $\langle \bar{u}u \rangle = \langle \bar{d}d \rangle = \langle \bar{s}s \rangle =: \phi_0$ . For a  $K^0$  transformation, as defined above, this state goes over into

$$\langle \bar{u}u \rangle' = \phi_0, \quad \langle \bar{d}d \rangle' = \langle \bar{s}s \rangle' = \cos \theta \phi_0, \quad \langle \bar{q} i\gamma_5 \tau_a q \rangle' = \sin \theta \hat{\theta}_a \phi_0, \quad a = 6, 7. \tag{11}$$

Obviously, the condensate with the quantum numbers of a kaon is maximal at  $\theta = \pi/2$ . Therefore, since in a color superconductor quark-antiquark states and diquark states can mix, maximally meson condensed states should correspond to  $\theta = \pi/2$  in this case as well. This is consistent with the effective Lagrangian description<sup>†</sup>. We will see that it is also confirmed by our numerical results.

### 3 Model

We consider an NJL-type Lagrangian with a point-like color-current interaction,

$$\mathcal{L} = \bar{q} (i\hat{\not{D}} - \hat{m}) q - g \sum_{a=1}^8 (\bar{q} \gamma^\mu \lambda_a q)^2, \tag{12}$$

where  $q$  denotes a quark field with three flavor and three color degrees of freedom,  $\hat{m} = \text{diag}_f(m_u, m_d, m_s)$ , and  $g$  is a dimensionful coupling constant.

---

<sup>†</sup>The angle  $\theta$  in Eq. (7) corresponds to the rotation angle  $\pi^a/f_\pi$  of the chiral field  $\Sigma = \exp(i\pi^a \lambda^a / f_\pi)$  which transforms like  $\Sigma \rightarrow L \Sigma R^\dagger$ , where  $L$  and  $R$  are the  $SU(3)$  matrices which transform the left and right handed quarks:  $q_L \rightarrow L q_L$ ,  $q_R \rightarrow R q_R$ . Hence, for  $L = R^\dagger$ , the transformation angle for the quarks is  $\theta/2$ , which is consistent with Eq. (3).

Performing a Fierz transformation into the particle-particle channel, the interaction part can be rewritten as

$$\mathcal{L}_{qq} = \frac{2}{3} g \sum_{A,A'} \left[ (\bar{q} i \gamma_5 C \tau_A \lambda_{A'} \bar{q}^T) (q^T C i \gamma_5 \tau_A \lambda_{A'} q) + (\bar{q} C \tau_A \lambda_{A'} \bar{q}^T) (q^T C \tau_A \lambda_{A'} q) \right] + \dots, \quad (13)$$

where we have listed only those terms which could potentially lead to a condensation in the channels  $s_{AA'}$  or  $p_{AA'}$ . The mean-field thermodynamic potential in the presence of these condensates is then given by

$$\Omega(T, \{\mu_{fc}\}) = -T \sum_n \int \frac{d^3 p}{(2\pi)^3} \frac{1}{2} \text{Tr} \ln \left( \frac{1}{T} S^{-1}(i\omega_n, \vec{p}) \right) + \frac{2}{3} g \sum_{A,A'} (|s_{AA'}|^2 + |p_{AA'}|^2) \quad (14)$$

where  $T$  is the temperature,  $\omega_n = (2n - 1)\pi T$  are fermionic Matsubara frequencies, and  $\{\mu_{fc}\}$  ( $f \in \{u, d, s\}$ ,  $c \in \{r, g, b\}$ ) denotes the set of chemical potentials related to the conserved flavor and color densities  $n_{fc}$  of the Lagrangian. They are often given as linear combinations of the chemical potentials  $\mu$ ,  $\mu_Q$ ,  $\mu_3$ , and  $\mu_8$  [23], which are related to the total quark number density  $n$ , the electric charge density  $n_Q$ , and the color densities  $n_3 = n_r - n_g$  and  $n_8 = (n_r + n_g - 2n_b)/\sqrt{3}$ , respectively ( $n_c := \sum_f n_{fc}$ ).

The inverse propagator in Nambu-Gorkov formalism reads

$$S^{-1}(p) = \begin{pmatrix} \not{p} + \hat{\mu}\gamma^0 - \hat{m} & \sum_{AA'} (\Delta_{AA'}^s \gamma_5 + \Delta_{AA'}^p) \tau_A \lambda_{A'} \\ \sum_{AA'} (-\Delta_{AA'}^{s*} \gamma_5 + \Delta_{AA'}^{p*}) \tau_A \lambda_{A'} & \not{p} - \hat{\mu}\gamma^0 - \hat{m} \end{pmatrix}, \quad (15)$$

with  $\hat{\mu} = \text{diag}_{fc}(\mu_{fc})$  and the scalar and pseudoscalar diquark gaps

$$\Delta_{AA'}^s = -\frac{4}{3} g s_{AA'}, \quad \Delta_{AA'}^p = -\frac{4}{3} g p_{AA'}. \quad (16)$$

In the following we restrict ourselves to the three scalar condensates of the CFL ansatz, Eq. (1), plus two pseudoscalar condensates, corresponding to either  $\pi^\pm$  ( $p_{57}$  and  $p_{75}$ ),  $K^\pm$  ( $p_{27}$  and  $p_{72}$ ), or  $K^0$  modes ( $p_{25}$  and  $p_{52}$ ). In other words, we allow for condensation only in one of these modes at a time, which is a reasonable assumption [11]. The inverse propagator, which is a  $72 \times 72$  matrix, can then be decomposed into a  $40 \times 40$  block and two  $16 \times 16$  blocks. Making use of the fact that the integrand in Eq. (14) does not depend on the direction of the 3-momentum, the dimensionality of the blocks can further be reduced by a factor one half. The determinants of the remaining  $20 \times 20$  and  $8 \times 8$  matrices and the Matsubara sum are evaluated numerically.

Until this point, the thermodynamic potential depends on our choice of the diquark gaps. As standard, the stable selfconsistent solutions are given by the values of  $\Delta_{AA'}^s$  and  $\Delta_{AA'}^p$  which minimize  $\Omega$ . In most cases below, however, we will restrict the minimization procedure to the subspace of condensates which can be obtained from the CFL solution ( $\Delta_{AA'}^p = 0$ ) via chiral rotations, Eq. (3) or Eq. (9), in order to compare our results with the effective Lagrangian approach.

## 4 Numerical results

In most of our numerical studies we adopt the model parameters of Ref. [22], namely a 3-momentum cut-off  $\Lambda = 600$  MeV and  $g\Lambda^2 = 2.6$  for the coupling constant. For comparison with the predictions of the effective Lagrangian approach we keep the quark masses as variable parameters. As before, we assume equal masses for up and down quarks,  $m_u = m_d =: m_q$ . All calculations are performed at zero temperature and at fixed  $\mu = 400$  MeV.

To have a well-defined starting point, we begin our analysis in the chiral limit,  $m_q = m_s = 0$  and with equal chemical potentials for all quarks, i.e.,  $\mu_Q = \mu_3 = \mu_8 = 0$ . For this case we find a CFL solution with  $\Delta_{22}^s = \Delta_{55}^s = \Delta_{77}^s = 104.2$  MeV. As expected, this is not a unique solution for the ground state, but an infinite set of degenerate ground states can be obtained via chiral rotations. In particular, any rotations in  $\pi^\pm$ ,  $K^\pm$ , or  $K^0$  direction leave the ground state free energy invariant.

Next we introduce a finite strange quark mass  $m_s = 120$  MeV, while leaving the up and down quarks massless. The explicit breaking of the  $SU(3)$  symmetry causes a slight asymmetry in the ground state, i.e., instead of an ideal CFL solution, Eq. (1), we get a 5% splitting of the gap parameters:  $\Delta_{22}^s = 105.4$  MeV and  $\Delta_{55}^s = \Delta_{77}^s = 100.7$  MeV. It turns out that the corresponding free energy is still invariant under chiral rotations into the  $\pi^\pm$  direction, whereas it becomes *disfavored*, if we perform a rotation into the kaonic directions. At first sight, this result seems to contradict the effective Lagrangian results, as summarized in Eqs. (5) - (7).

At this point we should notice that, by construction, the effective Lagrangian contains only colorless states (as a result of integrating out static gluons, see, e.g., Ref. [13]) whereas the above ground state of the NJL model is not color neutral. In fact, it is well known that the introduction of unequal masses in the CFL phase leads to colored solutions in NJL-type models, unless this is corrected for by introducing appropriate color chemical potentials [23]. This can be thought of as an effective way of simulating static gluon background fields. In the above example we need to introduce a chemical potential  $\mu_8 = -10.12$  MeV in order to obtain a color neutral CFL solution. This solution has a smaller splitting of the gaps,  $\Delta_{22}^s = 103.4$  MeV and  $\Delta_{55}^s = \Delta_{77}^s = 101.8$  MeV, and is about  $0.2$  MeV/fm<sup>3</sup> higher in free energy as the colored one.

However, the essential observation is that, restricting ourselves to color neutral solutions, the CFL state does no longer correspond to the ground state of the system if we allow for chiral rotations. This is illustrated in the left panel of Fig. 1 where the relative change of the free energy density is plotted as a function of the angle  $\theta$  for chiral rotations. While the rotations in pion direction (dashed line) still leave the free energy invariant, the kaonic transformations now lead to a reduction of  $\Omega$ . (Note that charged and neutral kaon solutions are degenerate under the present conditions.) Here the dotted line indicates the result of an axial flavor rotation ( $K^\pm$  or  $K^0$ ), and the solid line the result of an axial color rotation ( $K'^\pm$  or  $K'^0$ ). As one can see, the latter is more favored and symmetric about a minimum at  $\theta = \pi/2$ , while the former is less favored and slightly asymmetric.

This can be explained by the fact that, e.g., a  $K^0$  rotation transforms the larger  $s_{22}$ , in which  $u$  and  $d$  quarks are paired, into the  $us$  condensate  $p_{52}$ , whereas the smaller  $us$  condensate  $s_{55}$  is rotated into the  $ud$  condensate  $p_{25}$ . Hence, the number of strange

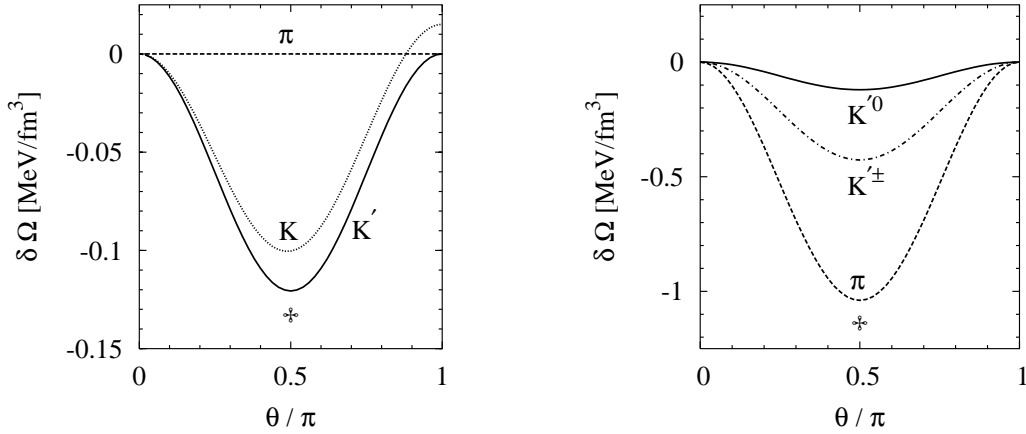


Figure 1: Relative change of the free energy density as a function of the chiral angle for  $m_u = m_d = 0$  and  $m_s = 120$  MeV. The calculations have been performed at  $\mu = 400$  MeV and  $\mu_Q = 0$  (left) or  $\mu_Q = -50$  MeV (right). The color chemical potentials have been adjusted to obtain color neutral solutions. The various lines correspond to different modes as indicated in the figure. The crosses indicate the free energy obtained by minimizing the thermodynamic potential for color neutral matter without restriction to chiral transformations.

quarks is larger at  $\theta = \pi$  than at  $\theta = 0$ , which explains why  $\theta = \pi$  is less favored. In a  $K'^0$  transformation, on the other hand,  $ud$  condensates remain  $ud$  condensates and  $ds$  condensates remain  $ds$  condensates, because axial color transformations do not change the flavor structure. Therefore the number of strange quarks at  $\theta = \pi$  is equal to the number of strange quarks at  $\theta = 0$ , and both states are degenerate.

None of the above results corresponds to the real minimum of the thermodynamic potential, because we have restricted ourselves to certain chiral rotations of the CFL solution without allowing for “radial” variations. This means, instead of freely varying the scalar and pseudoscalar condensates under consideration, we have linked them to the CFL solution and a single parameter  $\theta$ , e.g., as given in Eqs. (8) and (10) for the  $K^0$  or the  $K'^0$  case, respectively. If we abandon this constraint we find solutions with even lower free energies, indicated by the cross in the figure. These solutions are very similar to a  $K'$  state at  $\theta = \pi/2$ , in the sense that, e.g.,  $|\Delta_{22}^s| = |\Delta_{25}^p|$  and  $|\Delta_{55}^s| = |\Delta_{52}^p|$ , but the values of the  $ud$  gaps are slightly larger ( $74.2$  MeV =  $104.9$  MeV/ $\sqrt{2}$ ) and the values of the  $us$  gaps are slightly smaller ( $70.9$  MeV =  $100.2$  MeV/ $\sqrt{2}$ ) than the rotated CFL gaps.

In fact, in our context the  $K'$ -transformations should also be interpreted as certain “radial” transformations on top of the axial flavor transformation  $K$ , and not as axial color transformations. Note that, even in the chiral limit, axial color transformations, Eq. (9), are neither a symmetry of QCD nor of our NJL-model Lagrangian, Eq. (12). They are just a symmetry of the mean-field thermodynamic potential, as long as we restrict ourselves to the given set of diquark condensates. It will no longer be the case if, e.g.,  $\bar{q}q$  condensates are taken into account. In the present model, the difference between the  $K$  and  $K'$  transformations is due to the non-equality of the diquark condensates in the CFL phase (cf. Eqs. (8) and (10)). This is a higher-order effect, which is not taken into

account in the leading-order results of the effective Lagrangian approach. Hence  $K$  and  $K'$  transformations are in principle equally good starting points for a comparison with the effective theory. However, in some aspects the  $K'$  transformations behave more similar to the kaon modes in the effective theory since they are symmetric about  $\theta = \pi/2^\ddagger$ . Moreover, they come closer to the true minimum of the thermodynamic potential. Therefore, for most of quantitative studies in this article we perform  $K'$  transformations rather than  $K$  transformations. Note that for the pion modes there is no difference anyway.

In the right panel of Fig. 1 we show the result of a similar analysis, again for  $m_s = 120$  MeV, but now for a non-vanishing electric charge chemical potential  $\mu_Q = -50$  MeV. The color chemical potentials  $\mu_3$  and  $\mu_8$  have again been adjusted to ensure color neutrality at each point. Under these conditions all flavored Goldstone modes lead to a reduction of the free energy, but the pionic mode (dashed line) is the most favored one, followed by the charged kaons (dash-dotted). The neutral kaon is not sensitive to  $\mu_Q$  and shows the same behavior as in the left panel. As before, none of the modes corresponds to the real minimum of the thermodynamic potential one gets if the condensates are not constrained to certain chiral rotations. This free energy is again indicated by a cross in the figure.

At least qualitatively, the results presented in Fig. 1 are in good agreement with the predictions of the effective Lagrangian approach. For a more quantitative comparison we again restrict ourselves to chiral transformations of the CFL solution. In Fig. 2 we show the behavior of the free energy gain of the meson condensed solutions ( $\theta = \pi/2$ ) for massless up and down quarks as functions of  $\mu_Q$  (left panel) and  $m_s$  (right panel). At each point, the color chemical potentials  $\mu_3$  and  $\mu_8$  have been tuned to ensure color neutrality.

The left panel shows the behavior of  $\delta\Omega$  for the three Goldstone boson condensates  $\pi^\pm$ ,  $K'^\pm$ , and  $K'^0$  at fixed chiral angle  $\theta = \pi/2$  as functions of  $\mu_Q$  at fixed  $m_s = 120$  MeV. Since, according to Eqs. (5) to (7), we expect  $\delta\Omega_\pi$  to behave like  $\mu_Q^2$ , we plot the dimensionless ratio  $\delta\Omega/(\mu^2\mu_Q^2)$ . Indeed, our result for the pionic mode is constant to a very high degree (dashed line).  $\delta\Omega_{K'^0}$ , on the other hand, does not – and should not – depend on  $\mu_Q^2$ , and hence the corresponding curve (solid line) decreases like  $1/\mu_Q^2$  in the figure. Finally, the charged kaons behave more complicated. According to Eq. (6),  $\mu_{K^\pm}$  vanishes at  $\mu_Q = -m_s/(2\mu)$ , leading to a maximum in the free energy. Qualitatively, this is well reproduced in our model calculation (dash-dotted) line. In fact, in the  $\mu_Q$  interval between -13 MeV and -22 MeV,  $\delta\Omega_{K'^\pm}$  even gets slightly positive. This seems to indicate that the kaon is not exactly massless but has a small mass of about 5 MeV. Then, since the leading-order ( $\alpha_s^0$ ) effective theory predicts  $m_K = 0$  for  $m_q = 0$  (see Eq. (5)), this must be a higher-order effect due to interactions. There are, for instance, QCD corrections proportional to  $\alpha_s m_s^2$  [25], which have, however, the wrong sign. Nevertheless, there could be other terms which lead to the observed behavior. We will come back to this issue below.

For comparison, we also show the effective Lagrangian results for the free energy as given by Eqs. (5) to (7) (dotted lines). Here we treat  $f_\pi$  as a free parameter which

---

<sup>‡</sup>For instance, the color chemical potentials needed to neutralize the  $K'$  solution at the minimum at  $\theta = \pi/2$  satisfy the relation  $\mu_3 = \sqrt{3}\mu_8$ . This is in nice agreement with the ratio between the third and the eighth color component of the static gluon field,  $\phi_3^c = \sqrt{3}\phi_8^c$ , obtained in Ref. [24] for neutral CFL +  $K^0$  solutions. This relation does not hold for the  $K$  solution in our model.

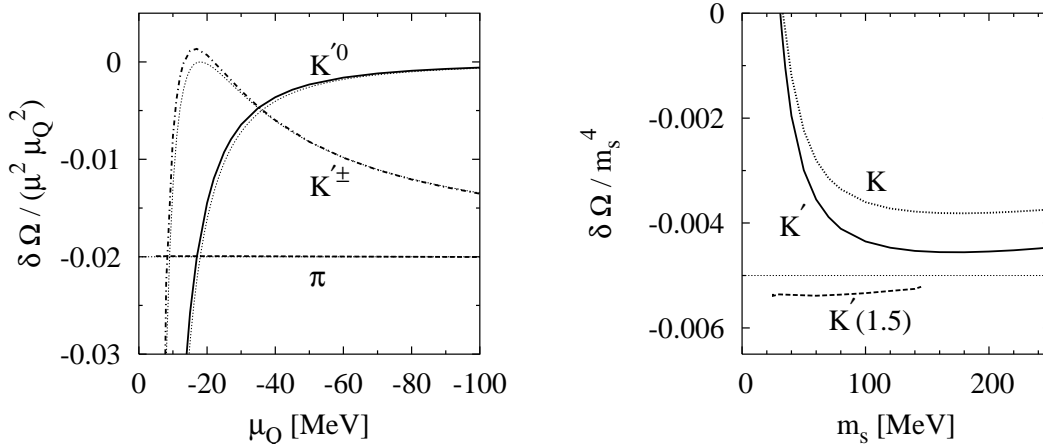


Figure 2: Free energy density difference between meson condensed phase ( $\theta = \pi/2$ ) and CFL phase ( $\theta = 0$ ) as functions  $\mu_Q$  (left) or  $m_s$  (right). The calculations have been performed for  $m_u = m_d = 0$  and at fixed  $\mu = 400$  MeV. The color chemical potentials have been adjusted to obtain color neutral solutions. In the left panel  $m_s = 120$  MeV, in the right panel  $\mu_Q = 0$ . The various lines correspond to different modes as indicated in the figure. The dashed curve labeled “ $K'(1.5)$ ” in the right figure has been calculated with a reduced coupling constant  $g\Lambda^2 = 1.5$ . The bold lines have been obtained within the present model while the thin dotted lines correspond to Eqs. (5) to (7) with  $f_\pi = 80$  MeV.

is fitted to reproduce the pion. We obtain  $f_\pi = 80$  MeV, which also gives reasonable fits to the kaons. The fitted value agrees quite well with the leading-order result  $f_\pi = \sqrt{(21 - 8 \ln 2)} \mu / (6\pi) = 83.4$  MeV. Again, there should be corrections to this formula due to the interaction. These could depend on the meson channel as well as on  $m_s$  and  $\mu_Q$ . Of course, meson masses and decay constants could be calculated explicitly within the NJL model, summing up  $q\bar{q}$  loops in Nambu-Gorkov formalism (which are essentially diquark loops) and coupling them to an external axial current. This is left for future work.

In the right panel of Fig. 2 the free energy of the kaonic modes ( $K$  and  $K'$ ) at  $\mu_Q = 0$  is shown as a function of  $m_s$ . For comparison we show again the result corresponding to Eqs. (5) to (7) for  $f_\pi = 80$  MeV (dotted line). Since according to these equations we expect  $\delta\Omega_K$  to behave like  $m_s^4$  we plot the ratio  $\delta\Omega/m_s^4$ . However, whereas for  $m_s \gtrsim 100$  MeV this ratio indeed is roughly constant, we find strong deviations at lower strange quark masses. In particular, below  $m_s = 31$  MeV the kaon modes are no longer favored.

Again, this indicates the presence of higher-order interaction effects. Note that the deviations from the  $m_s^4$  behavior show up in a regime where  $m_s$  is smaller than the CFL gap  $\Delta$ . Hence, terms of the order  $m_s^2\Delta^2$ ,  $\Delta^4$  or  $m_s^2\Delta^4/\mu^2$  [25], which are exponentially suppressed in the weak-coupling regime, could be parametrically comparable to  $m_s^4$ . To check this point, we redo the calculation with a reduced coupling constant,  $g\Lambda^2 = 1.5$ . The CFL gaps are then about 30 MeV, instead of  $\sim 100$  MeV which we had before. The resulting  $\delta\Omega$  for the  $K'$  mode is indicated by the dashed line in the figure. Obviously, this curve shows an almost perfect  $m_s^4$  behavior down to  $m_s = 25$  MeV and there is

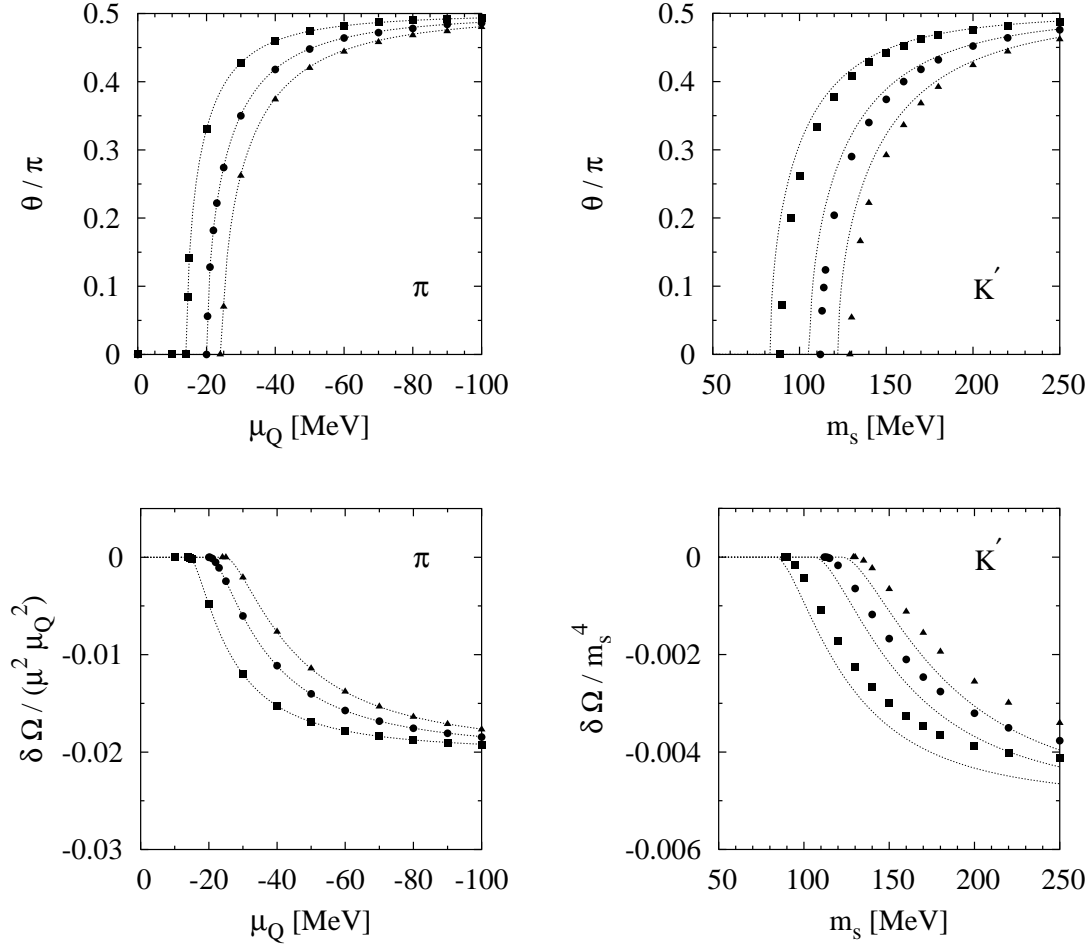


Figure 3: Chiral angle (upper panels) and corresponding free energy gain (lower panels) of meson condensed phases at  $\mu = 400$  MeV for non-vanishing light quark masses  $m_q$ . The full squares, circles, and triangles indicate the NJL model results for  $m_q = 5$  MeV, 10 MeV, and 15 MeV, respectively. The dotted lines are the corresponding results of Eqs. (5) to (7) with  $a = 0.169$  and  $f_\pi = 80$  MeV. Left: pion condensate for  $m_s = 120$  MeV and varying  $\mu_Q$ . Right: kaon condensate ( $K'$ ) for  $\mu_Q = 0$  and varying  $m_s$ .

no indication that kaon condensates become disfavored at small  $m_s$ . (Unfortunately, we cannot go to even smaller values of  $m_s$  because the numerical uncertainties become too large.) This means, there is at least numerical evidence that the effect seen with our original parameters is indeed due to interactions.

Finally, we consider non-vanishing masses for both, strange and non-strange quarks. Then, according to Eq. (5), the effective Goldstone masses become finite even at leading order, and  $m_s$  or  $\mu_Q$  have to exceed certain threshold values to enable Goldstone boson condensation. Our results are summarized in Fig. 3. The full squares, circles and triangles correspond to NJL-model calculations with  $m_q = 5$  MeV, 10 MeV, and 15 MeV, respectively.

In the two left figures we show the behavior of the pionic solutions for fixed  $m_s = 120$  MeV as functions of  $\mu_Q$ . In the upper panel the chiral angle  $\theta$  is shown which minimizes the free energy. As expected, this angle is zero for small values of  $|\mu_Q|$  and becomes non-zero above a threshold value which depends on the quark mass. This behavior can be described well by Eqs. (5) to (7) if we treat the constant  $a$  which enters into the expression for the meson masses as a free parameter. The dotted lines, which run almost perfectly through the points, have been obtained with  $a = 0.169$ . However, this is only about 1/3 of the leading-order result  $a = 3\Delta^2/(\pi^2 f_\pi^2)$  [12], if we take  $\Delta \sim 100$  MeV and  $f_\pi = 80$  MeV. Again, this discrepancy must be an interaction effect. Nevertheless, since in Fig. 2 we found the leading-order results to be in rather good agreement with the pion channel, a factor 3 in the present case is a bit surprising. To get some insight, we have again repeated the calculation with  $g\Lambda^2 = 1.5$ , i.e.,  $\Delta \sim 30$  MeV. For this case we find the fitted value for  $a$  to be about 2/3 of the leading-order prediction. This seems to indicate that the latter is reached asymptotically, but the convergence is relatively slow. A more systematic investigation of this point is certainly necessary.

In the lower left panel we display the free energy gain (for  $g\Lambda^2 = 2.6$ ). The dotted lines indicate the results of Eqs. (5) to (7), taking the previously fitted constants  $a = 0.169$  and  $f_\pi = 80$  MeV. Obviously, we obtain a perfect description of the NJL model results without refitting these constants.

In the right two figures the analogous quantities are shown for kaon ( $K'$ ) condensates at  $\mu_Q = 0$  as functions of the strange quark mass. The dotted lines correspond to Eqs. (5) to (7) with the values for  $a$  and  $f_\pi$  fitted in the pion channel. Obviously, the overall behavior is well reproduced, although the quantitative agreement is not as good as in the left two panels. In fact, the deviations are consistent with our earlier results: As one can see in the upper figure, the NJL-model results for the thresholds for kaon condensation are at somewhat higher values of  $m_s$  than the dotted lines suggest. This could again be explained by a positive correction term to the kaon mass beyond the leading order. Accordingly, the NJL-model results for  $\delta\Omega$  (lower right panel) are also shifted to higher values of  $m_s$  as compared with the dotted lines. On the other hand, for large  $m_s$ , the light quark masses become less relevant and the results approach the  $m_q = 0$  values of Fig. 2.

## 5 Summary and outlook

We have studied pion and kaon condensation in the CFL phase within an NJL-type model. To that end we have performed a mean-field calculation allowing for non-vanishing expectation values of certain scalar and pseudoscalar diquark condensates. Main focus of the present article was on the general principle. We have explicitly shown that Goldstone condensates, i.e., non-vanishing expectation values of pseudoscalar diquark condensates, develop in reaction to a finite strange quark mass or a finite electric charge chemical potential. In this context it was essential to introduce color chemical potentials to ensure color neutrality of the CFL and the CFL + Goldstone solutions.

More quantitatively, we found good over-all agreement of the NJL-model results with predictions obtained within chiral perturbation theory in the CFL phase to leading order in the interaction. The most intriguing exception is the coefficient  $a$ , which determines the

dependence of the Goldstone boson mass on the quark masses. Fitting this coefficient to our results, it turned out to be only one third of the leading order High Density Effective Theory value [12] if the coupling is relatively strong ( $\Delta \simeq 100$  MeV) and two thirds for a weaker coupling ( $\Delta \simeq 30$  MeV). The leading-order value may thus be reached at very weak couplings only, but this deserves further investigations. Apart from this point we found some deviations in the kaon sector which we also identified as interaction corrections to the leading order.

Having demonstrated the general consistency of the method, we should now extend our analysis to perform a more complete study of the phase structure of strongly interacting matter at high densities. In the present article, we have in most cases restricted the space of possible diquark condensates to certain chiral rotations, in order to facilitate the comparison with the effective theories. This restriction should be relaxed. As shown in Fig. 1, this can lead to a further reduction of the free energy.

The model should also be extended to include quark-antiquark condensates, like  $\langle \bar{u}u \rangle$ ,  $\langle \bar{d}d \rangle$ , and  $\langle \bar{s}s \rangle$ , which lead to density dependent effective quark masses and in this way could influence the phase structure considerably [22]. Now, in order to study Goldstone boson condensation, we also need to take into account the corresponding chiral partners,  $\langle \bar{q} i\gamma_5 \tau_a q \rangle$ . These condensates are the essential degrees of freedom to describe pion and kaon condensates in color non-superconducting phases, which have recently been studied in great detail in Ref. [18]. In the CFL phase, the dominant effects should be due to the diquark condensates, but nevertheless, quark-antiquark condensates could lead to important corrections. We should also note that our toy-model Lagrangian, Eq. (12), misses instanton effects, which could significantly contribute to the Goldstone boson masses [26]. Finally, it would be interesting to extend the analysis to the gapless CFL phase.

### Acknowledgments:

I am particularly grateful to Thomas Schäfer for many clarifying comments. I also thank Micaela Oertel, Krishna Rajagopal, Sanjay Reddy, Bernd-Jochen Schaefer, and Igor Shovkovy for valuable comments and discussions. Related work has been done independently by M. Forbes [27]. I also thank him for the subsequent communication which stimulated the study of the  $\Delta$  dependence of the results in the revised manuscript.

## References

- [1] M. Alford, K. Rajagopal, and F. Wilczek, Nucl. Phys. B 537 (1999) 443.
- [2] I.A. Shovkovy and L.C.R. Wijewardhana, Phys. Lett. B 470 (1999) 189.
- [3] T. Schäfer, Nucl. Phys. B 575 (2000) 269.
- [4] N. Evans, J. Hormuzdiar, S.D. Hsu, and M. Schwetz, Nucl. Phys. B 581 (2000) 391.
- [5] K. Rajagopal and F. Wilczek, “The Condensed Matter Physics of QCD”, in: B.L. Ioffe Festschrift *At the Frontier of Particle Physics / Handbook of QCD*, vol. 3, edited by M. Shifman, World Scientific, Singapore, 2001, pp. 2061–2151.

- [6] M. Alford, *Ann. Rev. Nucl. Part. Sci.* 51 (2001) 131.
- [7] T. Schäfer, hep-ph/0304281, to appear in the proceedings of the BARC workshop.
- [8] D.H. Rischke, *Prog. Part. Nucl. Phys.* 52 (2004) 197.
- [9] T. Schäfer, *Phys. Rev. Lett.* 85 (2000) 5531.
- [10] P.F. Bedaque and T. Schäfer, *Nucl. Phys. A* 697 (2002) 802.
- [11] D.B. Kaplan and S.Reddy, *Phys. Rev. D* 65 (2002) 054042.
- [12] D.T. Son and M.A. Stephanov, *Phys. Rev. D* 61 (2000) 074012; erratum *ibid D* 62 (2000) 059902.
- [13] R. Casalbuoni and R. Gatto, *Phys. Lett. B* 464 (1999) 111.
- [14] R. Casalbuoni, R. Gatto, and G. Nardulli, *Phys. Lett. B* 498 (2001) 179; erratum *ibid B* 517 (2001) 483.
- [15] D.K. Hong, *Phys. Lett. B* 473 (2000) 118.
- [16] S.R. Beane, P.F. Bedaque, and M.J. Savage, *Phys. Lett. B* 483 (2000) 131.
- [17] M. Buballa, hep-ph/0402234, *Phys. Rep.* in print.
- [18] A. Barducci, R. Casalbuoni, G. Pettini, and L. Ravagli, hep-ph/0410250.
- [19] M. Alford, C. Kouvaris, and K. Rajagopal, *Phys. Rev. Lett.* 92 (2004) 222001; hep-ph/0406137 to appear in *Phys. Rev. D*.
- [20] S.B. Rüster, I.A. Shovkovy, and D.H. Rischke, *Nucl. Phys. A* 743 (2004) 127.
- [21] K. Fukushima, C. Kouvaris, and K. Rajagopal, hep-ph/0408322.
- [22] M. Buballa and M. Oertel, *Nucl. Phys. A* 703 (2002) 770.
- [23] A. Steiner, S. Reddy, and M. Prakash, *Phys. Rev. D* 66 (2002) 094007.
- [24] A. Kryjevski, *Phys. Rev. D* 68 (2003) 074008.
- [25] A. Kryjevski, D. Kaplan, and T. Schäfer, hep-ph/0404290.
- [26] C. Manuel and M.H. Tytgat, *Phys. Lett. B* 479 (2000) 190.
- [27] M.M. Forbes, hep-ph/0411001.